Image Cover Sheet

CLASSIFICATION	SYSTEM NUMBER
UNCLASSIFIED	511940

TITLE

A Model of Cardiovascular Performance During Sustained Acceleration

System Number:

Patron Number:

Requester:

Notes:

DSIS Use only:

Deliver to:

98-P-91

A MODEL OF CARDIOVASCULAR PERFORMANCE DURING SUSTAINED ACCELERATION

C. Walsh[1]
S. Cirovic[2]
W. D. Fraser[3]

1. Department of Mechanical Engineering, Ryerson Polytechnic University, Toronto, Ontario, Canada
2. Institute for Aerospace Studies, University of Toronto, Toronto, Ontario, Canada
3. Defence and Civil Institute of Environmental Medicine, Toronto, Ontario, Canada

DCIEM, Building 54, ALSS
PO Box 2000
1133 Sheppard Avenue West
Toronto, Ontario, Canada
M3M 3B9

ABSTRACT

During aerial combat maneuvers, G_z can cause visual impairment or loss of consciousness (G-LOC). Anti-G suits, positive pressure breathing, and anti-G straining maneuvers reduce the risk of G-LOC. However, complex G-profiles are problematic. To assist in designing G-protective measures for such profiles, we are developing a model of human cardiovascular performance. We present preliminary results from a model that deals with the mechanical aspects of cardiovascular response to G_z. Physiological reflexes are neglected.

We consider a closed loop vascular network with a time varying elastance heart model. Blood flow is modeled by a one-dimensional (1-D) approximation: a pair of first order partial differential equations govern continuity and momentum. The blood pressure is determined by the external pressure and a tube law. The dominant physical phenomenon is wave propagation. The vasculature is modeled as a network of uniform flexible tubes. Valves are placed at the entrances and exits to the ventricles, and in the veins. The equations are solved numerically using a split coefficient matrix method. The algorithm is first order, and it is suited to wave propagation. The boundary conditions are implemented using the method of characteristics.

The results show cardiac output falling as G_z increases and rising again when G_z is reduced. Because there are no physiological reflexes, the central arterial pressure rises and falls with cardiac output, rather than being regulated to its physiological value. G-suit inflation, during periods of high G_z, returns the cardiac output to resting values when both the lower body and abdomen are covered. Protection is significantly reduced if only the lower body is covered. Simulations, in which G_z increases from 1 G to 4 G, are only plausible when there is at least one valve in the inferior vena cava.

1 INTRODUCTION

Rationale

The G_z values generated in aerial combat maneuvers are large enough to modify the blood circulation of the air crew. There is an increase in the hydrostatic pressure difference between the heart and each of the organs, and blood pools in the lower extremities, reducing venous return and cardiac output. Therefore, organs above the heart, particularly the eyes and brain, tend to experience lower blood pressure and lower perfusion. In unprotected individuals G-induced loss of consciousness, G-LOC, results at approximately 4.5 G. Although G-LOC is reversible, and causes no permanent damage in centrifuge experiments [4], when it occurs during combat maneuvers it poses grave risks to the air crew and aircraft [2].

The goal of the current project is to develop a numerical simulation of cardiovascular performance and cerebral perfusion. This simulation will give insights into the mechanisms of G-LOC during complex G-histories, and be of help in the design of advanced air crew life support systems.

Physiological background

For relaxed upright posture, during gradual onset rates of acceleration (GOR) cardiovascular reflexes, which are fully mobilised after approximately 20s [23], provide some protection. Typically, the carotid sinus reflex leads to peripheral vaso-constriction, increased heart rate and increased blood pressure [10], while the venous capacitance is reduced to maintain venous return [18]. As the body's regulatory mechanisms are overwhelmed, visual impairment occurs first [3]. This is because the high intra-ocular pressure makes the eyes more susceptible than the brain to low blood pressure. Thus, the normal sequence of events is peripheral vision loss (gray out) followed by total vision loss (blackout) and finally G-LOC. However, G-LOC can occur without preliminary visual impairment [25]. For GOR, the G-values at which these

phenomena occur become independent of time provided the cardiovascular reflexes are established. In contrast, for rapid onset rates (ROR), G-LOC occurs after an interval of approximately 4.2s that is independent of the G-rate or magnitude: cerebral blood flow ceases and the neurological cells must rely on their stored energy reserves.

Vascular networks

We are interested in closed loop vascular networks that incorporate a model of the heart [13, 14, 15, 17, 19, 22, 24]. The essential goal is to simulate cardiovascular performance with a set of material properties and governing equations. These are hyperbolic: the physics of the cardiovascular system is dominated by wave propagation.

The simulations with the greatest physiological detail are generally lumped parameter approximations. However, the lumping process typically leads to a spatial discretisation that is badly suited to wave propagation, and has poor stability characteristics for the parameter values of interest. One-dimensional (1-D) continuum models, in which the network element is a tube, permit difference schemes that can be tailored to the governing equations and boundary conditions [6, 7, 9, 17, 21]. The huge number of vessels present in the microcirculation cannot be modeled in detail. Instead, groups of small vessels in parallel are combined into equivalent tubes.

Approximate governing equations

1-D flow models focus on the bulk transport of blood mass and momentum through the vascular system. The governing equations, which can be derived from integral expressions of mass and momentum conservation, take the form

$$\frac{\partial V}{\partial t} = -\frac{\partial F}{\partial x} + S \tag{1}$$

where

$$V = \begin{pmatrix} A \\ U \end{pmatrix} \tag{2}$$

$$F = \begin{pmatrix} AU \\ U^2/2 + P_t/\rho \end{pmatrix} \tag{3}$$

$$S = \begin{pmatrix} \Psi \\ -\dfrac{8\pi\mu U n_v}{\rho A} - \dfrac{1}{\rho}\dfrac{dP_e}{dx} + g\cos\theta \end{pmatrix} \tag{4}$$

The first component of the vector equation (1) is the continuity equation, the second component is the momentum equation. Here t is time, x axial distance along the tube, A the tube cross-sectional area, U the mean flow speed, $P_t = P - P_e$ the transmural pressure, P the blood pressure, P_e the external pressure on a tube, and ρ the blood density. The source term S comprises: in the continuity equation, a leakage function Ψ; and, in the momentum equation, viscous dissipation, the gradient of external pressure, and the acceleration body force. The blood is assumed to be Newtonian

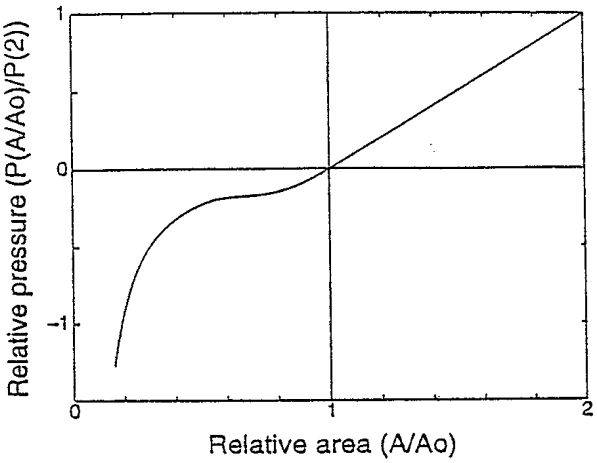

Figure 1: The tube law used by Sheng *et al.* [21].

with viscosity μ, and n_v parallel vessels are combined into one equivalent tube. θ is the angle between the tube axis and the body force.

Equation (1) comprises two equations in the three unknowns A, U, and P_t. A further approximation, called a tube law, expresses P_t as a function of the relative area A/A_0,

$$P_t = \mathcal{P}(A/A_0) \tag{5}$$

Here A_0 is the area of the vessel when P_t is zero. Corresponding expressions give the pressure as a function of volume for the heart chambers. Mathematically, the tube law closes the system of equation. Physically, it defines a long wave speed c as

$$c^2 = \frac{A}{\rho}\frac{\partial \mathcal{P}}{\partial A} \tag{6}$$

Common forms of $\mathcal{P}$ are either purely linear, or a combination of the similarity solution of Flaherty *et al.* [8], for $\mathcal{P} < 0$, with the linear law for $\mathcal{P} > 0$. Numerical algorithms generally demand some degree of differentiability, therefore a number of authors have smoothed the patch area as indicated in Figure 1 [5, 21].

There is a strong analogy with the equations of compressible gas and open channel flows [20], and a number of effective stable algorithms can be found in computational fluid dynamics publications [1, 11, 12]: the method of characteristics [6, 7], flux splitting [9], split coefficient matrix methods [1, section 6-4], and the MacCormack method [17, 21]. Although equation (1) is compact, the vascular geometry is complex and there are many internal boundaries. However, the method of characteristics provides a powerful tool for handling the boundary conditions.

Discussion

In general, there appears to be a strong consensus, amongst both the continuum and the lumped parameter closed loop

studies, regarding cardiac and arterial models. These incorporate a distributed arterial network with sound treatments of the arterial and cardiac mechanics, and of the baroreceptor reflexes [14, 15, 17, 19, 22, 24]. However, there is no such consensus regarding the model of the venous mechanics. The systemic veins may be lumped into a single element [14, 17, 22] or represented as a distributed network [15, 19, 24]. However, if autoregulation is modeled, control of venous compliance is also included [14, 17, 15]. Finally, none of the models cited in this paper includes lower body venous valves.

Objectives

The scope of the current study is limited to treating the mechanical and numerical issues that arise in a cardiovascular simulation. The model will be closed loop with a distributed venous and arterial network, and the simulation will allow G-histories, G-suit inflation, and positive pressure breathing. Given the preliminary nature of the work, no attempt will be made to produce a detailed cardiovascular model. However, the inclusion of anti-G protective measures demands that at least the cerebral, abdominal, and lower body capillary beds be differentiated. The new features introduced in this study are the use of a split coefficient matrix method, and inclusion of lower body vein valves.

2 METHODS

Program overview

The algorithm involves a large number of scalar function calls within nested loops. Problems of this type are most efficiently handled using compiled code. Our simulation is implemented in C. The hierarchy of structures used in the code is illustrated in Figure 2. At the top level is the flight environment, the principal members of which are an air crew list and a list of flight environment variables. Results are presented below for a single air crew member with the G-vector as the only flight environment variable. We propose

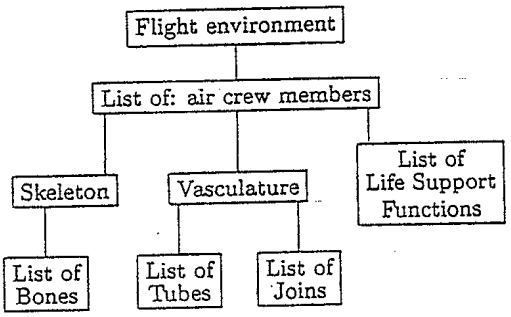

Figure 2: The higher level C structures used in the cardiovascular simulation.

to include cabin pressure as a flight environment variable in a later phase of the study that will deal with a lung model.

Each crew member comprises a vasculature, a skeleton, and a list of life support functions. We can currently simulate G-suit inflation, and the effects of positive pressure breathing on the systemic blood dynamics. Results are presented only for G-suit inflation. The skeleton comprises a list of 'bones': foot, calf, thigh, spine, neck, upper arm, and lower arm. For each of these we specify the rotation from the perpendicular to the floor of the environment, and thus the posture (sitting, standing, lying, etc.) of the crew member. The limbs are symmetrically placed, and results are presented below for the case of standing.

The vasculature is defined by first projecting all blood vessels onto a coronal plane, associating each blood vessel with a bone in the skeleton, and defining the angle between the bone and the vessel in the plane. With this information we calculate the orientation of each vessel in the flight environment, and the component of the G-vector acting along the axis of each vessel. Currently we assume that the G-vectors always lie in the sagittal plane of the crew member, and in the current study all bones are aligned with each other and the G-vector. The mechanical properties of the tubes are stored in the list of tubes, while the list of joins records whether inter-tube junctions have valves or resistances. In addition the tubes are oriented so that they have a beginning and an end, and both lists cross-reference each other: each tube has pointers to the join at its beginning and end; and each join has pointers to all of the tubes attached to it and flags to indicate whether it is the beginning or the end of the tube that is attached.

Physiological approximation

The vascular networks used in this paper are shown in Figure 3, where the circle denotes the left heart, the symbols > denote valves, and the arrows indicate the positive flow direction for each vessel. The line elements are blood vessels connecting the heart to three capillary beds represented in the diagram by the horizontal rectangles and in the model by pure resistances. The right heart and pulmonary circulation have been neglected, and the left heart simplified to a single chamber. These restrictions will be removed once the physiological reflexes are modeled. However, including the pulmonary circulation and all of the heart chambers will introduce no new mechanical problems, while substantially increasing the number of parameters that we need to estimate for the model. Furthermore, cardiac filling is largely passive, so that a plausible simulation can be obtained with no atria, and the principal mechanical determinants of venous return are associated with the systemic veins, which are modeled.

The vertical rectangles to either side of the network indicate two levels of G-suit coverage. The smaller one on the left covers only the lower body, while the larger one covers the lower body and abdomen. Each of the four horizontal

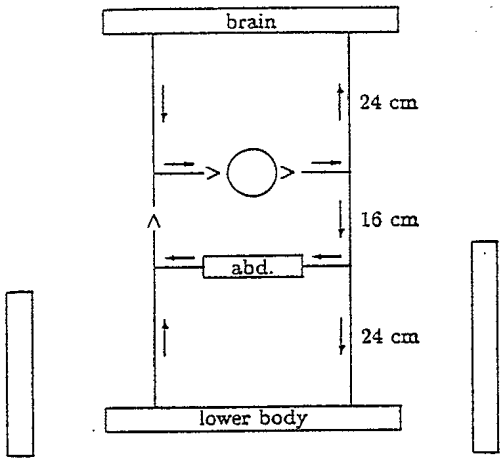

Figure 3: Vascular network

vessels is 8 cm in length. Some results will also be shown for a simpler network with no venous valve and one lower body capillary bed connected to the heart by an aorta and an inferior vena cava, each of length 40 cm. The vessel properties are the adapted from Sheng *et al.* [21].

G-suit

The G-suit model is based on the original Franks Flying Suit [16]: a water-filled garment covering the lower body and abdomen. We assume that, in the area of coverage, the G-suit exerts an external pressure equal to the hydrostatic pressure relative to the heart.

Valve model

All valves are passive. They open instantaneously under a forward pressure gradient, and are closed instantaneously, regardless of the pressure gradient, by back flow. When closed, valves do not leak. The valves have no equations of motion, but enter the governing equations through the tube boundary conditions. When a valve is open it has no effect. When it is closed it isolates the otherwise connected tubes and imposes a zero flow condition at the respective tube ends.

Heart model

The ventricular pressure P_v is defined as:

$$P_v = P_e + E_v(t)(\frac{V_v}{V_0} - 1) \quad (7)$$

$$E_v(t) = E_m + E_a \max(0, \sin(2\pi t/T)) \quad (8)$$

$E_v(t)$ is a variable elastance with period T, V_v is the ventricular volume, and V_0 is the ventricular volume at which $P_v - P_e = 0$.

When the central venous pressure (CVP) is greater than P_v, *i.e.*, during diastole, the mitral valve opens and the ventricle fills passively through a mitral resistor. When P_v is greater than the central arterial pressure (CAP), *i.e.*, during systole, the aortic valve opens and the heart empties actively, with the ejection flow speed determined by a momentum equation. The rate of filling or ejection in turn determines the rate of change of V_v. The heart properties are adapted from Ozawa [17].

Split coefficient matrix method

In the split coefficient matrix (SCM) method we rewrite equation (1) in terms of the Jacobian, A, of the flux vector and $\partial V/\partial x$.

$$\frac{\partial V}{\partial t} = -A\frac{\partial V}{\partial x} + S \quad (9)$$

where

$$A = \frac{\partial F}{\partial V} = \begin{bmatrix} U & A \\ c^2/A & U \end{bmatrix} \quad (10)$$

We can now diagonalise A using its eigenvalues $U \pm c$ and the array L of left eigenvectors, and split A into additive components $A_\pm$ that are associated with signals propagating in the positive and negative directions along the tube axis, [1, section 6-4].

$$L = \begin{bmatrix} c/A & 1 \\ -c/A & 1 \end{bmatrix} \quad (11)$$

$$A = L^{-1}\begin{bmatrix} U+c & 0 \\ 0 & U-c \end{bmatrix} L \quad (12)$$

and

$$A = A_+ + A_- \quad (13)$$

For supercritical flow, *i.e.*, $|U| > c$, one of the arrays $A_\pm$ will be zero the other will be equal to A. For subcritical flow, *i.e.*, $|U| < c$,

$$A_\pm = \frac{1}{2}(U \pm c)\begin{bmatrix} 1 & \pm A/c \\ \pm c/A & 1 \end{bmatrix} \quad (14)$$

For the discrete problem we use the notation V_i^n, where the superscript indicates the time level and the subscript the node number. $t^{n+1} = t^n + \Delta t$, where the time step Δt is the same for all tubes. On any tube the nodes are numbered sequentially with $x_{i+1} = x_i + \Delta x$, where the the space step Δx is constant on any tube, but can vary from tube to tube. We use a forward time difference, a backward spatial difference for the A_+ term, and a forward spatial difference for the A_- term. The difference equation is then

$$\frac{V_i^{n+1} - V_i^n}{\Delta t} = -A_+\left(\frac{V_i^n - V_{i-1}^n}{\Delta x}\right) - A_-\left(\frac{V_{i+1}^n - V_i^n}{\Delta x}\right) + S_i^n \quad (15)$$

Consistency, stability and convergence

The consistency of the discrete equation (15) with equation (1) is apparent from the very simple form of the difference expressions. On proving consistency by using Taylor series expansions of the differences, the truncation error is seen to be first order. A von Neuman stability analysis [11, Chapter 8] shows that the linearised form of equation (15) is stable provided the Courant-Friedrich-Lewy (CFL) condition is satisfied:

$$\frac{|c \pm U|\Delta t}{\Delta x} <= 1 \qquad (16)$$

Thus, we expect that the nonlinear equation (15) will be stable if the boundary conditions are treated correctly.

Initial conditions

The initial state for each simulation is $U_i^0 = 0$ everywhere with A_i^0 determined as follows: at arterial and venous roots, let the blood pressure be the anticipated mean blood pressure for that location; establish separate hydrostatic equilibria for the veins and arteries branching from their respective roots; use the tube laws to calculate the corresponding A_i^0; and assign volumes to each of the heart chambers. This leads to a pressure discontinuity at the capillary bed. This is desirable since the capillary flow begins immediately, reducing venous return artifacts during the first beat of the simulation.

Boundary conditions

The boundary conditions are applied using the method of characteristics following Hirsch [12, Chapter 19]. The principal boundary types are two-tube and multi-tube boundaries. All two-tube boundaries allow discontinuity of material and flow properties at the boundary and may include a boundary resistor and a valve. Two tube boundaries occur: at the heart; at the boundaries between tubes used to represent a larger vessel with varying properties; at the location of venous valves; and at the capillary bed in coarse vascular networks where we do not wish to treat the details of the vessels supplying the micro-circulation. Neither valves nor resistors can occur at multi-tube boundaries which represent arterial branching or venous convergence. Currently, we do not incorporate separation losses at any of the boundaries. Such losses can be modeled following Cancelli and Pedley [5] at sudden expansions, and Wolf [26] at branches.

Only the venous valve boundary is described for the case of subcritical flow. This case is illustrated in Figure 4. We assume that two tubes join at a valve with the positive direction for each tube going from left to right. The subscript $_l$ denotes valve boundary quantities from the left tube, and subscript $_r$ quantities from the right tube. Following Hirsch [12, section 16-4], we can define characteristic variables $w_\pm$ that are governed by first order ordinary differential equations (ODE) on characteristic paths $C_\pm$ as:

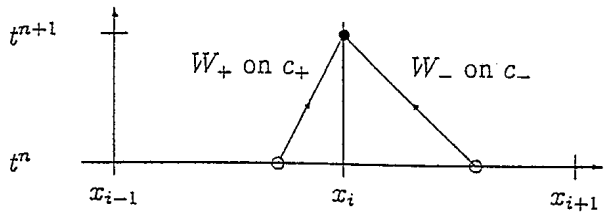

Figure 4: The method of characteristics applied at a subcritical boundary at $x = x_i$.

$$w_\pm = U \pm \int \frac{c}{A} dA = U \pm \mathcal{U}(A) \qquad (17)$$

with $C_\pm$ defined by

$$\frac{dx}{dt} = U \pm c \qquad (18)$$

Thus, a pair of characteristic paths meet at the valve at time t^{n+1}, with w_+ propagating from the left tube along C_+, and w_- propagating from the right tube along C_-. To first order the paths are straight lines, and we can use linear interpolation to determine the $w_\pm$ at time t^n, and then solve the governing ODE's to obtain estimates of the $w_\pm$ at time t^{n+1}. Now, using the two estimates for $w_\pm$, flow continuity and a momentum equation, we can solve for the values of A_l, U_l, A_r, and U_r. When the valve is open we have

$$\begin{aligned} U_l + \mathcal{U}(A_l) - w_+ &= 0 \\ U_r - \mathcal{U}(A_r) - w_- &= 0 \\ A_l U_l - A_r U_r &= 0 \\ P_l + \rho\frac{U_l^2}{2} - P_r - \rho\frac{U_r^2}{2} - U_l A_l R &= 0 \end{aligned} \qquad (19)$$

where R is a resistance to flow at the tube boundary. When the valve is closed we have

$$\begin{aligned} U_l &= 0 \\ \mathcal{U}(A_l) - w_+ &= 0 \\ U_r &= 0 \\ \mathcal{U}(A_r) + w_- &= 0 \end{aligned} \qquad (20)$$

In general these equations are nonlinear and cannot be solved analytically. Fortunately, the values of the unknowns at time t^n provide an excellent approximation to the values sought at t^{n+1}, and Newton's method converges very quickly.

Mass conservation

The SCM method does not enforce exact mass conservation, and numerical errors change the total blood volume. In this closed loop simulation, such errors lead to spurious changes in the blood pressure. Therefore, at each time step, when V_i^n and V_i^{n+1} are both still available, we adjust the volume

of each tube by estimating the error in the continuity equation using centred time and space differences. With this procedure the total blood volume varies by less than 0.005% during 16 cardiac cycles.

Model restrictions

Two simplifications have been made to reduce the computational costs associated with applying the method of characteristics at the boundaries: the vessel tube laws are assumed to be linear, corresponding to distended vessels, and the case of supercritical flow, *i.e.*, blood flow speed greater than the wave speed is not handled. The principal consequence of these restrictions is that the description of flow in the highly collapsed veins above the heart will be poor. Consequently, the mechanism for the action of positive pressure breathing cannot be effectively examined in the current study.

3 RESULTS

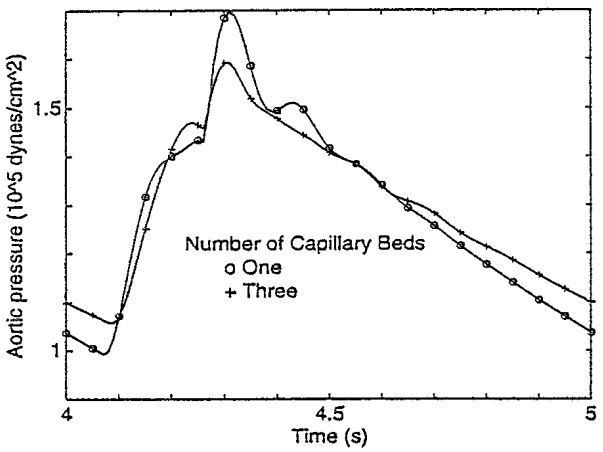

Figure 5: The effect of network complexity.

The aortic pressure is shown in Figure 5 during the fifth beat for the networks with one and three capillary beds. The principal difference between these results is the presence of large reflected waves in the one bed case. These are due to poor termination of the aorta, and are substantially reduced in the three bed case.

The G-history illustrated in Figure 6, where G_z=1.3 G for $5.5 \leq t \leq 11$, was applied to the one bed network, and the resulting ventricular volume history is shown in Figure 7. As expected, we see a drop in cardiac output during the period of elevated G_z. However, the magnitude of the drop is unreasonably large for such a small increase in G_z. It appears that the lower body veins defined by Sheng *et al.* [21] may be too compliant. Numerical experiments suggest that the vein stiffness in the lower body should be comparable with the arterial stiffness in order that the cardiac response

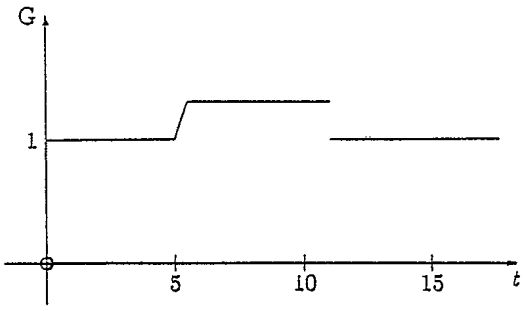

Figure 6: G-history, no G-suit inflation.

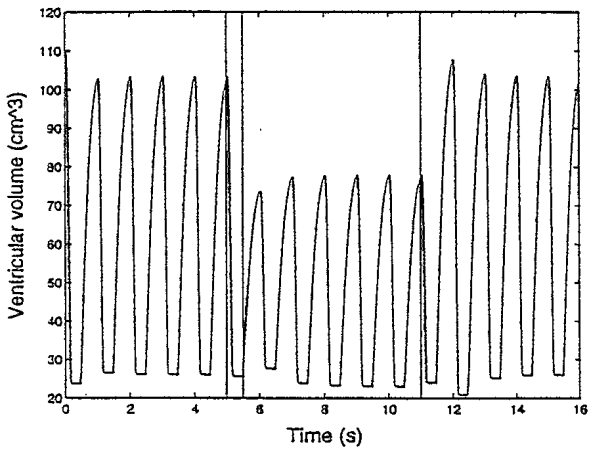

Figure 7: Ventricular volume for the one bed network subjected to the G-history in Figure 6.

to G be reasonable. The G-profiles in Figures 6 and 8 both involve discontinuities, and in neither case was there any numerical difficulty, suggesting that the algorithm is robust.

The G-history illustrated in Figure 8, where $G_z = 4\,G$ for $5.5 \leq t$, and the G-suit is inflated at $t = 11$, was applied to the three bed network with the lower body vein stiffnesses raised to arterial levels. The resulting CAP and CVP are shown in Figure 9. In performing the simulation it was apparent that a valve was needed in the inferior vena cava to prevent high speed back flow in that vessel. With the valve present a reasonable simulation was obtained with a large drop in CAP and also cardiac output. Note that in a real cardiovascular system the baroreceptor reflexes would quickly act to return CAP to the normal range. Here we see that inflating the G-suit raises the CAP, and that the suit covering the lower body and abdomen is markedly superior to the one that covers only the lower body.

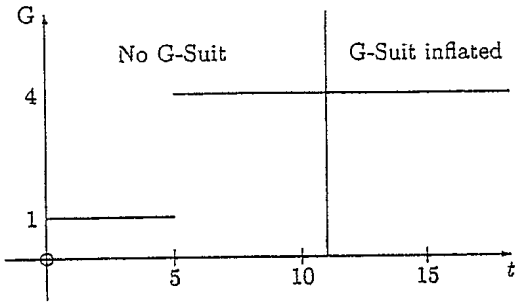

Figure 8: G-history, with G-Suit inflation.

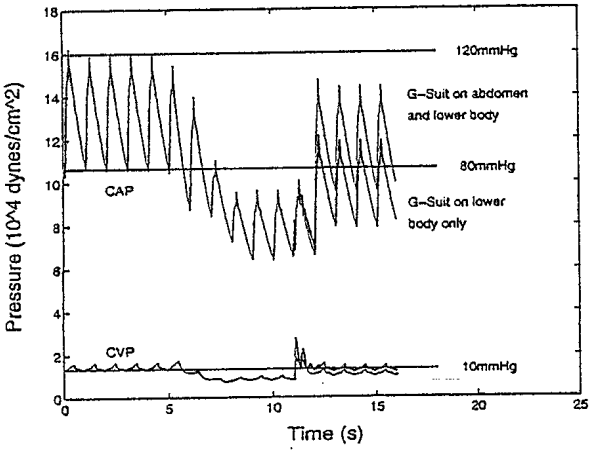

Figure 9: CAP and CVP for the three bed network subjected to the G-history of Figure 8.

4 CONCLUSIONS

The SCM method with a method of characteristics boundary treatment provides a robust and effective algorithm for cardiovascular simulations. At higher values of $G_z$it appears that at least one valve is needed in the inferior vena cava to maintain physiologically reasonable behaviour, and that the commonly used vessel material models are too compliant for the lower body veins. It is possible that the distended vessels have moved to a much stiffer operating point on the nonlinear vein response, or that the stiffness of the lower body vessels is dominated by the surrounding muscles and not their own properties. Both of these possibilities suggest that direct determination of *in vivo* vein tube laws should be made over the physiological range of transmural pressures.

When a G-suit is inflated during high $G_z$it markedly improves cardiovascular performance, and coverage of both the abdomen and lower body produces much better results than coverage of only the lower body.

5 ACKNOWLEDGEMENTS

This work has been generously supported by the Canadian Department of National Defence. DCIEM Research Paper No. 98-P-XX

6 REFERENCES

[1] Anderson, D. A., J. C. Tannehill, and R. H. Pletcher (1984). *Computational Fluid Mechanics and Heat Transfer.* Hemisphere.

[2] Banks, R. D., M. L. Brush, and H. L. Wright (1997). Operational implications of push-pull effect. In *The Aerospace Medical Association, 68th. Annual Scientific Meeting, Chicago Illinois.*

[3] Burton, R. R., S. D. Leverett, and E. D. Michaelson (1974). Man at high sustained +Gz acceleration: A review. *Aerospace Medicine 45*(10), 1115–1136.

[4] Cammarota, Jr., J. P. (1994). *A Dynamic Percolation Model of the Central Nervous System Under Acceleration (+Gz) Induced Ischemic/Hypoxic Insult.* Ph. D. thesis, Drexel University.

[5] Cancelli, C. and T. J. Pedley (1985). A separated-flow model for collapsible tube oscillations. *Journal of Fluid Mech. 157*, 375 – 404.

[6] Collins, R. and J. Maccario (1979). Blood flow in the lung. *Journal of Biomechanics 12*, 373–395.

[7] Collins, R. and E. Mateeva (1991). Assessment of physiological requirements for protection of the human cardiovascular system against high sustained gravitational stresses. In *High Altitude and High Acceleration Protection for Military Aircrew*, AGARD Conference Proceedings, 516, pp. 18–1 – 18–12.

[8] Flaherty, J. E., J. B. Keller, and S. I. Rubinow (1972). Post-buckling behaviour of elastic tubes and rings with opposite sides in contact. *SIAM Journal of Applied Mathematics 23*, 446–455.

[9] Gaffie, D., P. Quandieu, P. Liebart, D. Cohen-Zardy, T. Daumas, and A. Guillaume (1991). Circulatory biomechanics effects of accelerations. In *High Altitude and High Acceleration Protection for Military Aircrew*, AGARD Conference Proceedings, 516, pp. 19E–1 – 19E–15.

[10] Gauer, O. H. and G. D. Zuidema (1961). *Gravitational Stress in Aerospace Medicine.* Little, Brown & Co.

[11] Hirsch, C. (1990a). *Numerical Computation of Internal and External Flows*, Volume 1. John Wiley & Sons.

#511940